Talanta 233 (2021) 122566

Contents lists available at ScienceDirect

Talanta

journal homepage: www.elsevier.com/locate/talanta

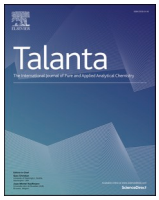

Terminal protection of peptides by interactions with proteins: A "signal-on" peptide-templated gold nanocluster beacon for label-free protein detection

Qian Wen [a,*], Si-Li Yi [c], Qin-Lu Lin [a], Li-Juan Tang [b], Jian-Hui Jiang [b,**]

[a] Hunan Key Laboratory of Grain-oil Deep Process and Quality Control, College of Food Science and Engineering, Central South University of Forestry and Technology, Changsha, Hunan, 410004, PR China

[b] Address Here State Key Laboratory of Chemo/Biosensing and Chemometrics, College of Chemistry and Chemical Engineering, Hunan University, Changsha, 410082, PR China

[c] Institute of Food Safety and Environment Monitoring of Photocatalysis on Energy and Environment College of Chemistry, Fuzhou University, Fuzhou, 350116, PR China

ARTICLE INFO

Keywords:
Terminal protection
Peptide-templated
Gold nanocluster
Protein
Detection

ABSTRACT

Characterization of the protein-peptide interactions are a critical for understanding the functions and signal pathways of proteins. Herein, a new finding of universal terminal protection that protein bind specifically with peptide and provide a protective coating to prevent peptide hydrolysis in the presence of peptidase. On the basis of this mechanism, we first reported a novel label-free fluorescence biosensor strategy that utilizes the protection of specific terminal protein on peptide-templated gold nanocluster (AuNCs) beacon for the detection of proteins. The fluorescence quenching of peptide-templated AuNCs can be effectively inhibited with increasing concentration of the specific protein, exhibiting a satisfactory sensitivity and selectivity toward protein with the detection limit of MDM2 and gp120 are 0.0019 U/mL and 0.0012 U/mL, respectively. The developed label-free fluorescence biosensor strategy provides new ideas to detect and screen protein for analyzing protein-peptide interaction in biomedical applications.

1. Introduction

Protein−peptides interactions form the basis of various cellular processes. More than 40% of the protein interaction pathways are estimated to be mediated by the interactions between proteins and peptides [1,2]. Characterization of the proteins−peptides interactions are a critical for understanding the functions and signal pathways of proteins [3,4]. Identification of protein-binding peptides also creates the possibility for designing new peptide-based probes or drugs that can facilitate the interrogation of target protein–peptides interactions [5,6].

In order to screen proteins that interact with specific peptides for the further analysis of proteins−peptide interactions, routine detecting techniques include electrophoresis [7], mass spectrometry [8], surface plasmon resonance [9] and resonance rayleigh scattering method [10]. However, these methods usually require sophisticated instrumentation and involve tedious assay optimization, or complicated separation and treatment for target protein. Hence, it is highly desirable to develop a novel strategy for sensitive, rapid and convenient detection and screening of target protein in biology and clinical theranostics [11,12].

Peptide-based fluorescence biosensors provide an attractive option for the detection of protein because of its high sensitivity, excellent temporal resolution and flexible functionality. However, the design of peptide sensors for protein recognition is challenging because of the lack of generic biochemical property discriminating between protein-binding peptides and non-binding ones. An important and useful mechanism for the peptide-based sensor development is conformational switching [13]. On interacting with its cognate target, the peptide probe undergoes a conformational change, altering the distance between a pair of fluorescence donor and acceptor labels and thus inducing a detectable resonance energy transfer signal [14–16]. A significant progress in this direction is peptide beacons [17,18], and recently developed peptide nucleic acid beacons [19,20].

In the previous study, we reported peptide-templated AuNCs beacon as biosensor for the detection of protein post-translational modification enzymes [21]. Herein, we first reported a label-free fluorescence biosensor strategy for the detection and screening of protein based on peptide-templated AuNCs beacon to the best of our knowledge. The gold clusters were oxidized as the substrate peptide was hydrolyzed by

* Corresponding author.
** Corresponding author.
E-mail address: wenqian_1104@163.com (Q. Wen).

https://doi.org/10.1016/j.talanta.2021.122566
Received 25 February 2021; Received in revised form 23 May 2021; Accepted 26 May 2021
Available online 8 June 2021

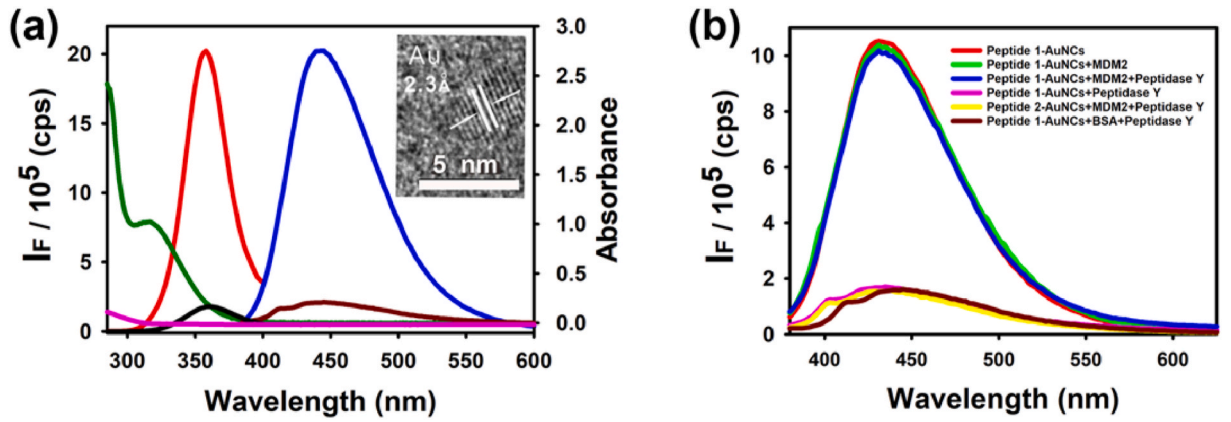

Fig. 1. (a) High resolution TEM image of peptide **1**-templated AuNCs. (b) UV–Visible absorption spectra of AuNCs with peptide 1 template (green) and non-template (pink). (c) Fluorescence excitation and emission spectra of AuNCs with peptide 1 template (red and blue) and non-template (black and brown). (d) Fluorescence spectral responses of peptide 1-templated AuNCs in different system. (For interpretation of the references to colour in this figure legend, the reader is referred to the Web version of this article.)

peptidase, the fluorescence of peptide-templated AuNCs was gradually quenched. When template peptide interacts specifically with protein that can bind on the terminal of peptide and prevent peptide hydrolysis in the presence of peptidase, inhibiting the fluorescence quenching of AuNCs. This protein-responsive fluorescent AuNCs can be as a simple and useful biosensor to detect and screen proteins which interact with a specific peptide for the deeper investigation of proteins−peptides interactions. In this work, we choose MDM2 and gp120 as protein model to verify the feasibility of the biosensors. Both MDM2 and gp120 are known to be tightly implicated in tumor metastasis, virus invasion and are most potential diagnostic biomarkers therapeutic targets.

2. Experimental sections

2.1. Materials and reagents

MDM2, gp120, Carboxypeptidase Y, BSA and $HAuCl_4{\cdot}3H_2O$ were purchased from Sigma-Aldrich (Missouri, USA) and 3-mercaptopropionic acid (MPA) was from ACROS (New Jersey, USA). All other chemicals were of analytical grade and obtained from Sinopharm Chemical Reagent Co. Ltd (Shanghai, China). The peptides were synthesized by a solid phase method from GL Biochem Co. Ltd. (Shanghai, China). All solutions were prepared using ultrapure water, which was obtained through a Millipore Milli-Q water purification system (Billerica, MA, USA) and had an electric resistance >18.3 MΩ. The glassware was washed with aqua regia (HCl: HNO_3 in a volume ratio of 3:1), and then rinsed with ultrapure water for three times.

2.2. Synthesis and characterization of peptide-templated AuNCs

In a mixture of 200 μL of 62 μM peptide aqueous solution, 1.5 mL of 50 mM $HAuCl_4$ aqueous solution and 1.5 mL methanol, 300 μL of 30 μM MPA aqueous solution was added under stirring on a magnetic stirrer. The pH value of the mixture was adjusted with 150 M NaOH (~60 μL) to pH 8. Then, the mixture was stirred for 10 min followed by the addition of 300 μL of 1 M $NaBH_4$ that was freshly prepared in ice-cooled water. The reaction mixture was stirred for another 10 min to allow the formation of the peptide-templated AuNCs. The resulting AuNCs (~3.6 mL) were concentrated and washed with ultrapure water for three times by ultrafiltration using a centrifugal filter unit (Amicon Ultra-0.5 mL with MWCO of 3000, Millipore) so as to remove excessive peptide and MPA. The concentrated AuNCs were diluted with ultrapure water to 1.8 mL.

The fluorescence spectra were measured at room temperature in a 100 μL quartz cuvette on a Fluorolog-Tau-3 spectrofluorometer (Jobin Yvon Inc., NJ) with the slit set to be 5 nm for both the excitation and the emission. The ultraviolet–visible (UV–vis) absorption spectra were measured using a UV-2550 spectrometer (Shimadzu, Japan) with a wavelength interval of 2 nm. The morphologies of the AuNCs were obtained using a JEOL JEM-2100 transmission electron microscope (TEM). The capillary electrophoresis experiment was recorded using a capillary electrophoresis system equipped with UV absorption detection (P/AGE MDQ, Beckman, Germany) in 50 mM borate running buffer (pH 9.2) under an applied potential of 15 kV and detected at 254 nm for 30 min at 25 °C (the quartz capillary diameter: 75 μm, effective length: 30 cm).

2.3. Peptide-templated AuNCs probe for the detection of MDM2

In a typical assay, in a 100 μL reaction buffer containing 50 nM peptide 1-templated AuNCs, 16.5 mM Tris-HCl (pH 8.0), 50 mM sodium chloride, 1 mM EDTA and 20% DMSO, 5 μL of MDM2 of a given concentration was added. The mixture was incubated at 37 °C for 30 min to allow a complete binding reaction. After the reaction, the pH value of the mixture was adjusted with 15 M HCl (~2 μL) to pH 6.75. Then, the 2 μL of 1U/ml carboxypeptidase Y was added to the mixture at 25 °C for 25 min. The resulting solution was immediately subjected to fluorescence spectral measurements. Time-dependent fluorescence responses of the reaction were taken at a time interval of 30 s. The fluorescence spectra were recorded in the emission wavelength range from 390 to 600 nm with an excitation wavelength at 350 nm.

The control experiments were performed under the same conditions except the replacement of a given reagent by a control reagent, such as replacing peptide **1**-templated AuNCs by an equal volume of AuNCs templated by another peptide, or replacing MDM2 by an equal volume of another protein.

2.4. Peptide-templated AuNCs probe for the detection of gp120

In a typical assay, in a 100 μL reaction buffer containing 50 nM peptide **2**-templated AuNCs, 50 mM PBS (pH 7.4), 5 μL gp120 of a given concentration was added. The mixture was incubated at 37 °C for 45 min to allow a complete deacetylation reaction. After the reaction, the pH value of the mixture was adjusted with 15 M HCl (~1 μL) to pH 6.75. Then, 2 μL of 1 U/ml carboxypeptidase Y was added to the mixture at 25 °C for 25 min. The resulting solution the resulting solution was immediately subjected to fluorescence spectral measurements. Time-dependent fluorescence responses of the reaction were taken at a time interval of 30 s. The fluorescence spectra were recorded in the emission wavelength range from 390 to 600 nm with an excitation wavelength at 340 nm.

The control experiments were performed under the same conditions

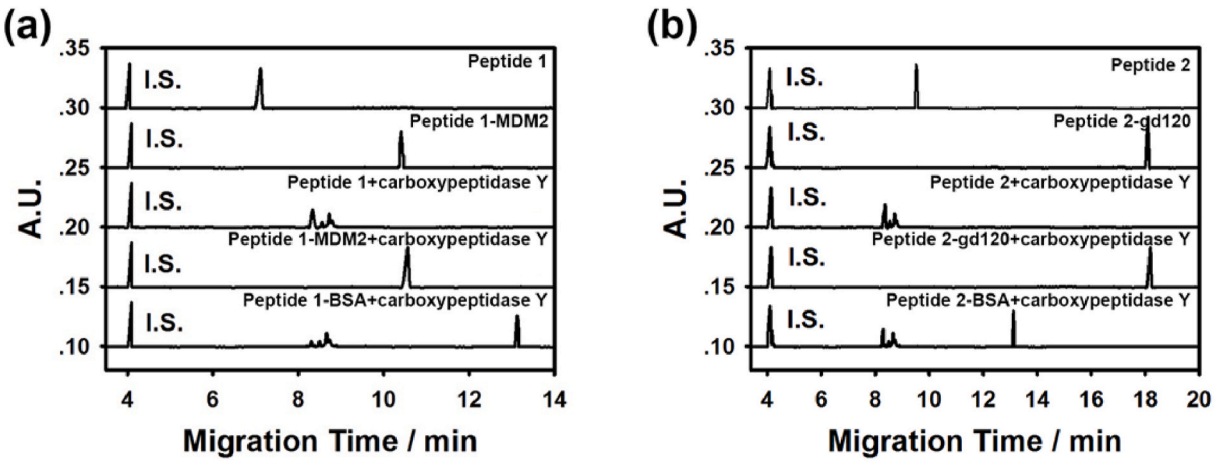

Fig. 2. (a) Electrophoretograms of 2 μM peptide-1, 2 μM peptide-1 binding MDM2, 2 μM peptide-1 plus 2 μL of 1 U/ml carboxypeptidase Y, 2 μM peptide-1 binding MDM 2 with 2 μL of 1 U/ml carboxypeptidase Y and 2 μM peptide-1 with BSA plus 2 μL of 1 U/ml carboxypeptidase Y. (b) Electrophoretograms of 2 μM peptide-2, 2 μM peptide-2 binding gd120, 2 μM peptide-2 plus 2 μL of 1 U/ml carboxypeptidase Y, 2 μM peptide-2 binding gd120 with 2 μL of 1 U/ml carboxypeptidase Y and 2 μM peptide-2 with BSA plus 2 μL of 1 U/ml carboxypeptidase Y. Internal standard is 4 μM peptide-3.

except the replacement of a given reagent by a control reagent, such as replacing peptide **2**-templated AuNCs by an equal volume of peptide **1**-templated AuNCs, replacing gp120 by an equal volume of other antibody.

3. Results and discussion

3.1. Synthesis and characterization

Peptide templated AuNCs can be easily prepared according to previous report, because peptide has two cysteine amino acids at N-terminal and exhibits high affinity to gold, providing a structure-defined template for the growth of AuNCs [22,23]. The sequences of the synthesized peptides are given in Table S1. The high-resolution transmission electron microscopy image shows that lattice fringes (~2.3 A) of AuNCs are coincide with the interplanar spacing of the (111) crystal plane of face-centered cubic Au, implying the synthesized peptide-templated AuNCs are Au_8 clusters with surface peptide (Fig. 1a) [24,25].

3.2. Spectral characteristics of peptide-templated AuNCs

The spectral characteristics of peptide 1-templated AuNCs were recorded and are shown in Fig. 1b–c. Peptide 1-templated AuNCs shows a broad absorption band with an onset near 400 nm and an intensive blue fluorescence. The emission maximum appears at 450 nm and the excitation wavelength at 360 nm. However, the non-templated AuNCs were synthesized in the absence of peptide 1 exhibited a weak blue emission with a maximum at 450 nm, which is significantly lower than that of peptide 1-templated AuNCs, implying the essential role of the peptide template for highly emission AuNCs. The enhanced emission indicated that the peptide template actually provided a protective coating for AuNCs, inhibiting oxidation of Au and O_2-mediated fluorescence quenching.

An interesting finding was that the peptides tethering on the prepared AuNCs could continue to serve as effective substrate for specific protein, and the fluorescence of peptide-template AuNCs would be quenched with the hydrolysis of the peptide. Take peptide 1-templated AuNCs as an example, the fluorescence spectral responses of peptide 1-templated AuNCs in different system are shown in Fig. 1d. It can be clearly found that peptide 1-templated AuNCs shows a higher emission intensity, but the emission intensity obviously decreased after the peptide **1**-templated AuNCs reacted with 2 μL of 1 U/ml carboxypeptidase Y. Notably, we incubated the peptide **1**-templated AuNCs with MDM2, the fluorescence signal of peptide **1**-templated AuNCs have no significant decrease in the presence of carboxypeptidase Y. This result illustrates that the fluorescence quenching of peptide **1**-templated AuNCs was specifically originated from the hydrolyzation of the peptide 1 by carboxypeptidase Y. The presence of MDM2 provided a protective coating.

For peptide 1 and inhibited the hydrolysis of peptide 1. To further validated whether the terminal protection was selective to protein, we incubated BSA with peptide **1**-templated AuNCs, the emission intensity of peptide **1**-templated AuNCs significantly reduced. On the other hand, we used peptide 2 as peptide template for control experiments, the synthesized peptide 2-templated AuNCs also exhibited strong fluorescence emission under the excitation of 360 nm light. However, a remarkable fluorescence quenching was observed both peptide 2-templated AuNCs linking MDM 2 and BSA after being treated with carboxypeptidase Y. These observations implied that peptide-templated AuNCs biosensor exhibited excellent selectivity, it can be used as fluorescence biosensor for the specific detection of protein.

3.3. Mechanism of sensing studies

In order to unveil the fluorescence response mechanism of peptide templated-AuNCs and verify the specific terminal protective effect of protein for peptide. First, electrophoresis was used for the investigation of protein terminal protection for peptide hydrolysis. The peaks appearing in the electrophoretograms were exclusively arising from the peptide and its bind products due to absorption coefficients of the proteins at 254 nm and limited working concentrations involved in the experiments [26]. This feature give us permission to directly visualize the hydrolyzation status of the peptides. Electrophoretograms for the peptide under the carboxypeptidase Y treatment were shown in Fig. 2a. A sharp peak for the peptide **1** and peptide **1** linked MDM2 were observed, but two individual peaks are observed for the carboxypeptidase Y treated peptide 1, meaning a complete hydrolyzation of the peptide 1 sequence by carboxypeptidase Y. The migration time of the MDM2 linked peptide 1 obviously extended after interacted with carboxypeptidase Y. These results indicate that MDM2 would interact with exposed surface silanol groups on the capillary wall of peptide 1 and prolonged migration time. Even if MDM2 linked peptide 1 complex undergo extensive hydrolyzation by carboxypeptidase Y over 1 h, the electrophoresis peaks of the complex have no obvious change, clearly confirming that hydrolysis of the peptide 1 by carboxypeptidase Y was

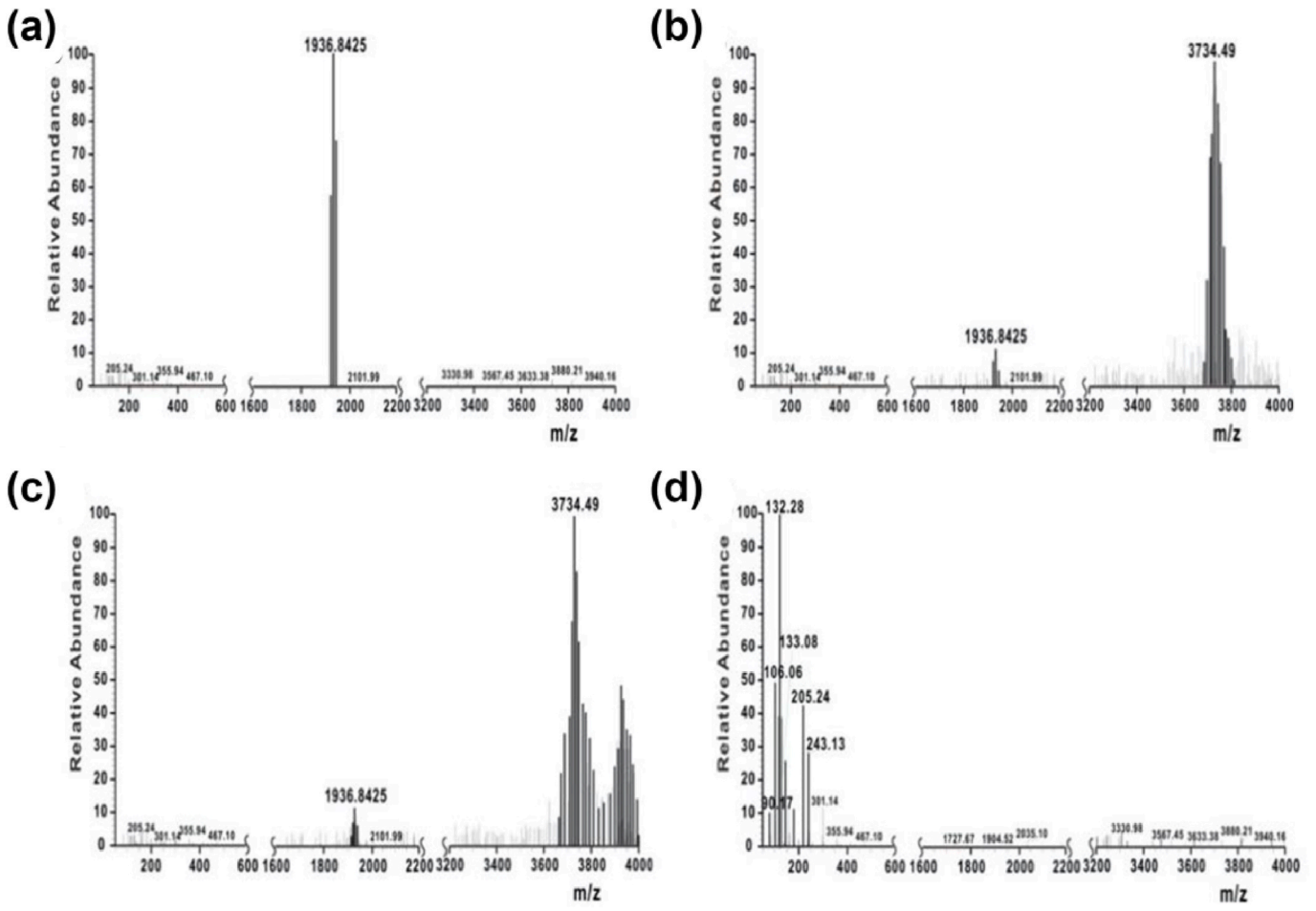

Fig. 3. ESI MS spectra for peptide **1** templated AuNCs (50 nM) obtained after decomposing the AuNCs cores. (a) before linked with MDM2, (b) after linked with MDM2, (c) linked with MDM2 and plus 2 μL of 1 U/ml carboxypeptidase Y, (d) reaction with 2 μL of 1 U/ml carboxypeptidase Y and without MDM2. MDM2 concentration was 60 nM.

prevented by the MDM2 binding event. The electrophoretogram also exhibits two peaks for these two mononucleotides in the presence of BSA, which indicate that BSA did not play a protective role in the hydrolysis of peptide 1, because the specific sequence of amino acids is the prerequisite for the binding of peptides with proteins [27]. The same phenomenon that we can see from peptide 2 linked gp120, illustrating that the method of protein terminal protection for peptide has significant specificity (Fig. 2b).

Next, we further used ESI-MS to investigate protein terminal protection for peptide through peptidase mediated hydrolysis reaction (Fig. 3). The ESI-MS mass spectra for the peptide 1-templated AuNCs show intense peak at 1936.842 Da and 3734.49 Da, respectively, before and after the peptide 1-templated AuNCs linked with MDM2. With the carboxypeptidase Y added into the liquid of peptide 1-templated AuNCs without linked with MDM2, many small peaks around the 132.28 Da were observed. Notably, it still only a peak at 3734.492 Da after the carboxypeptidase Y added into the liquid of peptide 1-templated AuNCs linked with MDM2.

The above results demonstrate that the presence of MDM2 provides protection to the peptide 1 from carboxypeptidase Y hydrolysis. The same phenomenon can be found in carboxypeptidase Y mediated hydrolysis reaction between the peptide 2-templated AuNCs and gp120 (Fig. S1). In addition, fluorescence anisotropy measurement results show that only peptide 1-templated AuNCs with carboxypeptidase Y exhibited decreased values of fluorescence anisotropy (Fig. S2). This result, presumably attributed to the hydrolysis reaction changed viscosity microenvironment for the AuNCs. Thus, we could presume a

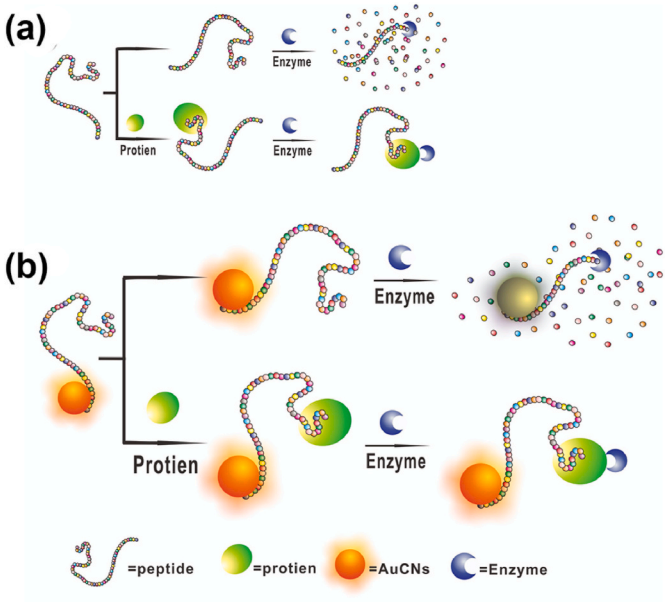

Scheme 1. Illustration of the mechanism for the peptide-templated AuNCs as a label-free sensor for protein.

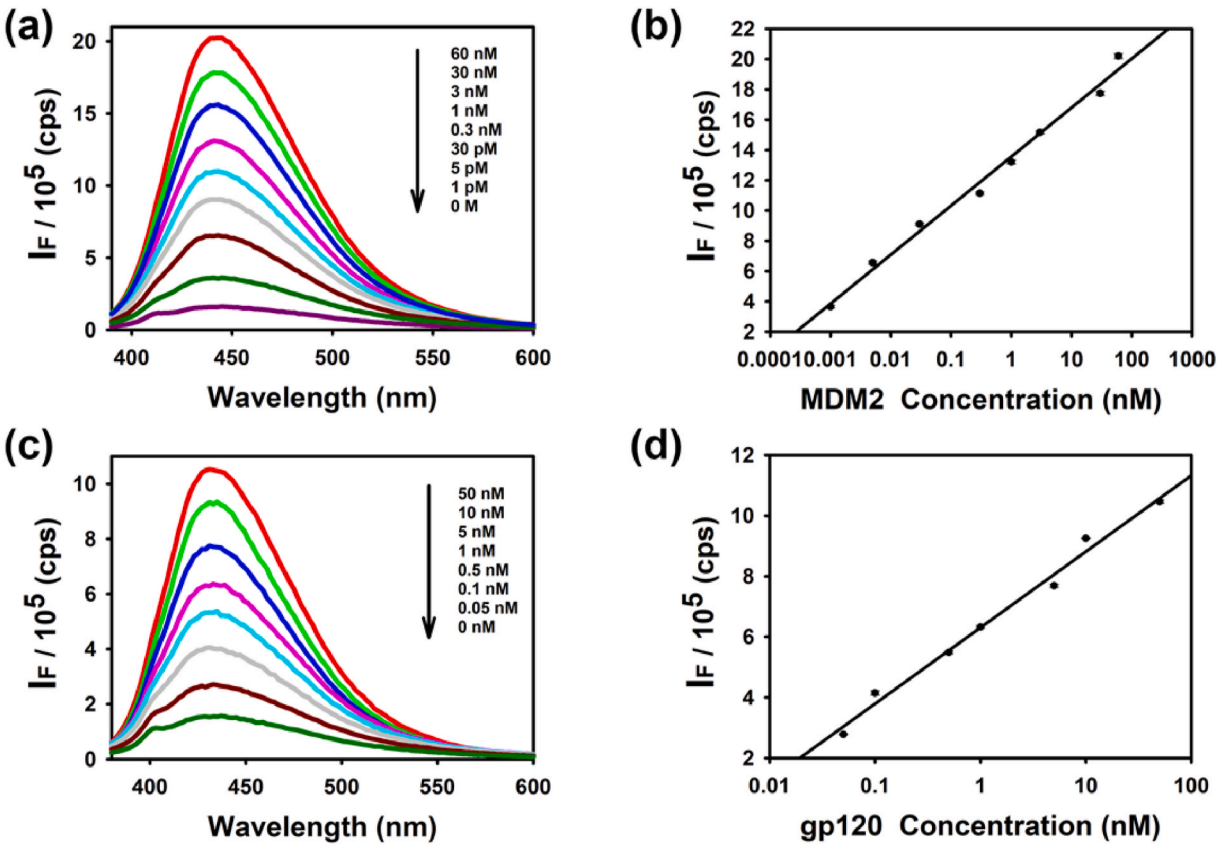

Fig. 4. (a) Fluorescence spectral responses of peptide 1-templated AuNCs to MDM2 of varying concentrations with plus 2 μL of 1 U/ml carboxypeptidase Y. (b) Fluorescence peak intensities versus MDM2 concentrations in logarithmic scale. (c) Fluorescence spectral responses of peptide 2 templated AuNCs to gp120 of varying concentrations with plus 2 μL of 1 U/ml carboxypeptidase Y. (d) Fluorescence peak intensities versus gp120 concentrations in logarithmic scale Error bars indicated SDs across four repetitive assays.

mechanism of the peptide-templated AuNCs fluorescence biosensor strategy for the specific detection of protein combined above results, as shown in Scheme 1.

3.4. *The application of peptide-templated AuNCs for detecting protein*

Since these two peptide-templated AuNCs biosensors show high selectivity toward protein, they were next applied for the detection of protein. First, fluorescence spectral responses were studied during the reaction between the peptide 1-AuNCs (50 nM) and 2 μL of 1 U/ml carboxypeptidase Y with two different concentrations of MDM2 (Fig. S3). The fluorescence of the peptide 1-templated AuNCs is gradually quenched over time and reached plateau within 25 min at room temperature. As expected, the lower concentration MDM2 have shown higher fluorescence quenching efficiency. The main reason is that higher concentration of MDM2 could provide terminal protection for peptide 1 to a large extent, thereby reducing the hydrolysis of peptide 1 by carboxypeptidase Y.

Next, the fluorescence spectral responses of the peptide-templated AuNCs to protein (MDM2 and gd120) of varying concentrations are depicted in Fig. 4. Peptide 1-templated AuNCs exhibits weak emission in the presence of carboxypeptidase Y, whereas a dynamically increased fluorescence intensity with increasing the concentration of MDM2 was observed, the fluorescence responses displayed a linear correlation to the logarithm values of MDM2 concentration in a range from 1 pM to 60 nM. According to the 3σ/k (where σ is the standard deviation of the zero standards, k is the slope for the range of the linearity used [28], the limit of detection (LOD) was calculated to be 0.0019 U/mL. Peptide 2-templated AuNCs was used for the detection of gp120 (Fig. 4c–d). The result was similar to the peptide 1-templated AuNCs, the fluorescence quenching degree of peptide 2-templated AuNCs gradually decreased with the increased of the gp120 concentration, the LOD is 0.0023 U/mL in a range from 1 pM to 50 nM. Such a low detection limit and wide dynamic range implied that this label-free biosensor have a high response sensitivity to proteins. In addition, the emission of peptide 1-templated AuNCs after storage 30 days at room temperature also demonstrates high stability of our method (Fig. 4S). Therefore, this strategy is expected to have potential in the detection and screening of proteins for deep investigation of protein-peptide interaction in biomedical applications.

4. Conclusion

In summary, we report a label-free fluorescence biosensor strategy for the specific detection of protein based on peptide-templated AuNCs beacon. The protein-responsive property of peptide-templated AuNCs were successfully demonstrated using MDM2 and gp120, exhibiting a satisfactory sensitivity and selectivity with the detection limit of MDM2 and gp120 are 0.0019 U/mL and 0.0012 U/mL, respectively. We believe that it will provide new ideas to detect and screen protein for analyzing protein-peptide interaction in biomedical applications.

Declaration of competing interest

The authors declare that they have no known competing financial interests or personal relationships that could have appeared to influence the work reported in this paper.

Acknowledgments

This work was supported by the National Natural Science Foundation of China (21505040) and the Natural Science Foundation of Hunan Province (2019JJ51004).

Appendix B. Supplementary data

Supplementary data to this article can be found online at https://doi.org/10.1016/j.talanta.2021.122566.

Credit author statement

Author contributions Qian Wen: Project design, Preparation of materials, Analysis, Writing – original draft. Sili Yi: Project design, Analysis, Writing. Qin-Lu Lin: Preparation of materials, Fluorescence analysis. Li-Juan Tang: protein analysis. Jian-Hui Jiang: Writing: Review & Editing.

References

[1] T.A. Cardote, A. Ciulli, Cyclic and macrocyclic peptides as chemical tools to recognise protein surfaces and probe protein-protein interactions, ChemMedChem 11 (8) (2016) 787–794.
[2] C. Katz, L. Levy-Beladev, S. Rotem-Bamberger, T. Rito, S.G. Rudiger, A. Friedler, Studying protein-protein interactions using peptide arrays, Chem. Soc. Rev. 40 (5) (2011) 2131–2145.
[3] P.L. Yang, R.J. Whelan, Y.W. Mao, A.W. Lee, C.C. Su, R.T. Kennedy, Multiplexed detection of protein-peptide interaction and inhibition using capillary electrophoresis, Anal. Chem. 79 (2007) 1690–1695.
[4] C.H. Lu, J. Li, X.L. Zhang, A.X. Zheng, H.H. Yang, X. Chen, G.N. Chen, General approach for monitoring peptide-protein interactions based on graphene-peptide complex, Anal. Chem. 83 (19) (2011) 7276–7282.
[5] L.G. Milroy, T.N. Grossmann, S. Hennig, L. Brunsveld, C. Ottmann, Modulators of protein-protein interactions, Chem. Rev. 114 (9) (2014) 4695–4748.
[6] S. Xie, A.Y.H. Wong, S. Chen, B.Z. Tang, Fluorogenic detection and characterization of proteins by aggregation-induced emission methods, Chemistry 25 (23) (2019) 5824–5847.
[7] P.L. Yang, R.J. Whelan, E. Jameson, J.K. Kurzer, L.S. Argetsinger, C.C. Su, A. Kabir, A. Malik, R.T. Kennedy, Capillary electrophoresis and fluorescence anisotropy for quantitative analysis of peptide-protein interactions using JAK2 and SH2-Baˆ as a model system, Anal. Chem. 77 (2005) 2482–2489.
[8] V. Baghalabadi, A.A. Doucette, Mass spectrometry profiling of low molecular weight proteins and peptides isolated by acetone precipitation, Anal. Chim. Acta 1138 (2020) 38–48.
[9] M.B. Villiers, S. Cortes, C. Brakha, J.P. Lavergne, C.A. Marquette, P. Deny, T. Livache, P.N. Marche, Peptide-protein microarrays and surface plasmon resonance detection: biosensors for versatile biomolecular interaction analysis, Biosens. Bioelectron. 26 (4) (2010) 1554–1559.
[10] X. Zhang, S. Yang, R. Jiang, L. Sun, S. Pang, A. Luo, Fluorescent molecularly imprinted membranes as biosensor for the detection of target protein, Sensor. Actuator. B Chem. 254 (2018) 1078–1086.
[11] I. Chakraborty, G. Rahamim, R. Avinery, Y. Roichman, R. Beck, Nanoparticle mobility over a surface as a probe for weak transient disordered peptide-peptide interactions, Nano Lett. 19 (9) (2019) 6524–6534.
[12] M. Retout, H. Valkenier, E. Triffaux, T. Doneux, K. Bartik, G. Bruylants, Rapid and selective detection of proteins by dual trapping using gold nanoparticles functionalized with peptide aptamers, ACS Sens. 1 (7) (2016) 929–933.
[13] C. Mueller, T.N. Grossmann, Coiled-coil peptide beacon: a tunable conformational switch for protein detection, Angew Chem. Int. Ed. Engl. 57 (52) (2018) 17079–17083.
[14] X. Cai, W. Wei, Y. Bi, Z. Liu, Z. Bai, J. Lei, J. Xiao, An intrinsically nontrimerizing peptide probe for specifically targeting pathological collagen in connective tissues, Adv. Funct. Mater. 30 (42) (2020).
[15] C. Zhai, C.L. Schreiber, S. Padilla-Coley, A.G. Oliver, B.D. Smith, Fluorescent self-threaded peptide probes for biological imaging, Angew Chem. Int. Ed. Engl. 59 (52) (2020) 23740–23747.
[16] H.M. Wang, J. Liu, A. Han, N.N. Xiao, Z.S. Xue, G. Wang, J.F. Long, D.L. Kong, B. Liu, Z.M. Yang, D. Ding, Self-Assembly-induced far-red: near-infrared fluorescence light-up for detecting and visualizing specific protein peptide interactions, ACS Nano 8 (2014) 1475–1484.
[17] D. Maity, C. Schmuck, Fluorescent peptide beacons for the selective ratiometric detection of heparin, Chemistry 22 (37) (2016) 13156–13161.
[18] D. Maity, K.I. Assaf, W. Sicking, C. Hirschhauser, W.M. Nau, C. Schmuck, A selective cucurbit[8]uril-peptide beacon ensemble for the ratiometric fluorescence detection of peptides, Chemistry 25 (57) (2019) 13088–13093.
[19] P. Fu, S. Xing, M. Xu, Y. Zhao, C. Zhao, Peptide nucleic acid-based electrochemical biosensor for simultaneous detection of multiple microRNAs from cancer cells with catalytic hairpin assembly amplification, Sensor. Actuator. B Chem. 305 (2020).
[20] Y. Zhao, A. Sarkar, X. Wang, Peptide nucleic acid based tension sensor for cellular force imaging with strong DNase resistance, Biosens. Bioelectron. 150 (2020) 111959.
[21] Q. Wen, Y. Gu, L.J. Tang, R.Q. Yu, J.H. Jiang, Peptide-templated gold nanocluster beacon as a sensitive, label-free sensor for protein post-translational modification enzymes, Anal. Chem. 85 (24) (2013) 11681–11685.
[22] M. Yu, C. Zhou, J. Liu, J.D. Hankins, J. Zheng, Luminescent gold nanoparticles with pH-dependent membrane adsorption, J. Am. Chem. Soc. 133 (29) (2011) 11014–11017.
[23] J.P. Xie, Y.G. Zheng, J.Y. Ying, Protein-directed synthesis of highly fluorescent gold nanocluster, J. Am. Chem. Soc. 131 (2009) 888–889.
[24] L. Yan, Y. Cai, B. Zheng, H. Yuan, Y. Guo, D. Xiao, M.M.F. Choi, Microwave-assisted synthesis of BSA-stabilized and HSA-protected gold nanoclusters with red emission, J. Mater. Chem. 22 (3) (2012) 1000–1005.
[25] M.S. Finnin, J.R. Donigian, A. Cohen, V.M. Richon, R.A. Rifkind, P.A. Marks, R. Breslow, N.P. Pavletich, Structures of a histone deacetylase homologue bound to the TSA and SAHA inhibitors, Nature 401 (1999) 188–193.
[26] W. Zhan, Z. Zhen, J.H. Jiang, G.L. Shen, R.Q. Yu, Terminal protection of small-molecule-linked DNA for sensitive electrochemical detection of protein binding via selective carbon nanotube Assembly, J. Am. Chem. Soc. 131 (2009) 12325–12332.
[27] Y.S. Chang, B. Graves, V. Guerlavais, C. Tovar, K. Packman, K.H. To, K.A. Olson, K. Kesavan, P. Gangurde, A. Mukherjee, T. Baker, K. Darlak, C. Elkin, Z. Filipovic, F.Z. Qureshi, H. Cai, P. Berry, E. Feyfant, X.E. Shi, J. Horstick, D.A. Annis, A. M. Manning, N. Fotouhi, H. Nash, L.T. Vassilev, T.K. Sawyer, Stapled alpha-helical peptide drug development: a potent dual inhibitor of MDM2 and MDMX for p53-dependent cancer therapy, Proc. Natl. Acad. Sci. U. S. A. 110 (36) (2013) E3445–E3454.
[28] J. Zhao, L. Yang, Y. Dai, Y. Tang, X. Gong, D. Du, Y. Cao, Peptide-templated multifunctional nanoprobe for feasible electrochemical assay of intracellular kinase, Biosens. Bioelectron. 119 (2018) 42–47.